JOURNAL OF GUIDANCE, CONTROL, AND DYNAMICS
Vol. 27, No. 4, July–August 2004

Missile Autopilot Design Using Discrete-Time Variable Structure Controller with Sliding Sector

A. A. Powly and M. Seetharama Bhat
Indian Institute of Science, Bangalore 560012, India

In this paper a discrete variable structure controller with sliding sector is designed for tracking the lateral acceleration command for a dual-input air-to-air missile. A new algorithm is developed for the variable-width sliding-sector design by considering the dissipativeness property of the system. The width of the sliding sector is based on the norm of the linear uncertain system state and the reference input. The switching surface design is based on the reduced-order dynamics. The control law is designed such that the state trajectory from any initial point is driven into the sliding sector around the equilibrium point in the vicinity of the the switching surface σ_k and thereafter remains inside it. The discrete sliding condition considered is $\|\sigma_{k+1}\| < \|\sigma_k\|$. Inside the sliding sector, the closed-loop system is dissipative with a linear control law. The uncertain missile plant with matched and mismatched uncertainty is considered, and the conditions on the norm-bound of the uncertainty are given for robust stability in the sense of Lyapunov. Simulation results of the missile autopilot are also included to show the efficacy of the proposed controller.

Nomenclature

C_t	=	tracking output matrix
$f(x, k, u)$	=	matched uncertainty
h	=	upper bound on mismatched uncertainty
r_k	=	reference command
$sgn()$	=	signum function
$\mathcal{J}_d$	=	sliding sector
u_k	=	m-dimensional control input
V_k	=	Lyapunov function
x_k	=	n-dimensional state variable
y_{tk}	=	tracking output
Γ	=	augmented system input matrix
ΔA_p	=	plant uncertainty in continuous time domain
δ_k	=	sliding sector function
ρ	=	upper bound on the matched uncertainty
σ_k	=	switching function
Φ	=	augmented plant matrix
$\|\ \|$	=	Euclidean norm for vectors and spectral norm for matrices

I. Introduction

THE variable structure control approach is well known for its robustness properties and is a powerful tool for controlling uncertain dynamical systems. Continuous time variable structure control (VSC) systems and its applications have been extensively studied in the literature over the past four decades.[1–4] The VSC is a special class of nonlinear control strategy characterized by a discontinuous feedback control that changes the controller structure upon reaching certain user-specified manifold called switching surface or sliding surface $\sigma(t)$. The central feature of VSC is the sliding mode (SM), during which the system state is constrained to lie on a sliding surface where the system dynamics are merely determined by the dynamics of the switching surface (SS), which is of lower order. Hence the system is invariant in the sliding mode, and the motion

A. A. Powly was born in Kerala, India. She graduated from Calicut University in 1986 with B. Tech in electrical engineering and received a M. Tech degree in control systems from the University of Kerala in 1988. She worked as Lecturer in Bangalore University from 1988 to 1998. She is a Research Scholar in Aerospace Engineering, at Indian Institute of Science, Bangalore and is currently working in the area of variable structure control-based flight control systems for aircraft and missiles. Her research interests are discrete variable structure control with sliding mode with state and output feedback, nonlinear control, robust multivariable control.

M. Seetharama Bhat obtained a Ph.D. degree in aerospace engineering from Indian Institute of Science, Bangalore, India in 1982. He has been on the faculty of aerospace engineering since October 1982. Currently he is Professor in Aerospace Engineering and also Convener of ISRO-IISc Space Technology Cell. M. S. Bhat has research interests in the area of dynamics and control of aerospace vehicles, guidance of rockets and missiles, estimation, control of smart structures, dynamics and control of mini– and micro–air vehicles.

Received 28 January 2002; revision received 3 November 2003; accepted for publication 30 December 2003.

of the state trajectories are less sensitive to parameter variations and disturbances.

Owing to the widespread use of digital controllers, VSC designed on the basis of continuous system is usually implemented by a digital computer with a certain sampling interval. This can enhance chattering with the predesigned SM and even can cause instability with large gains.[5] In practice, fast sampling is used, but this can lead to fatigue of actuator components. Theoretically, discrete variable structure control systems (VSCS) cannot be obtained from their continuous counterpart by means of simple equivalence.[6] The discrete-time variable structure control systems (DVSCS) differ from continuous-time VSCS mainly in the determination of switching hyperplane and the satisfaction of the reaching conditions. In the case of DVSCS, the control input is computed at discrete instants and applied to the system by holding the control input as a constant throughout the sampling interval. Thus switching takes place only at regular discrete instants. This is in contrast to the continuous-time systems, where the switching of the control structure is made as soon as the state trajectory crosses the switching hyperplane. Hence the DVSCS are not necessarily robust with respect to perturbations, if the design philosophy for continuous time systems is extended to the discrete-time case. Also the existence of SM is not guaranteed in the presence of uncertainties. The discrete sliding mode design philosophy thus requires modifications.

The stability of the discrete-time sliding mode control systems is investigated by Sarpturk et al.[7] and gives a necessary and sufficient condition for the existence of the discrete sliding mode (DSM) in multi-input/multi-output (MIMO) systems as

$$|\sigma_{ik+1}| < |\sigma_{ik}| \qquad i = 1 : m \tag{1}$$

($m =$ the number of inputs) in the neighborhood of $\sigma_k = 0$. The conditions for the existence of DSM and a design procedure for sliding lattice that ensures robust stability of sliding motion are given by Koshkouei and Zinober.[8] Instead of the conventional switching surface, in discrete-time case a switching region or a sliding lattice exists in the neighborhood of the sliding surface. Furuta[5] uses the Lyapunov function $V_k = \frac{1}{2}(\sigma_k)^2$ for single-input/single-output (SISO) systems and obtains the condition, which is equivalent to Eq. (1), as

$$\sigma_k \Delta\sigma_{k+1} < -\tfrac{1}{2}(\Delta\sigma_{k+1})^2 \tag{2}$$

In this paper, assuming all states are available, a linear reference input dependent SS of the form $\sigma_k = Sx_k - S_r r_{k-1}$ is used in the discrete variable structure controller design. The candidate Lyapunov function is taken as $V_k = \sigma_k^T \sigma_k$, and the discrete sliding condition[8] considered is

$$\|\sigma_{k+1}\| < \|\sigma_k\| \tag{3}$$

Edwards and Spurgeon[9] use a similar SS, $\sigma(t) = S_1 x_1 + S_2 x_2 - S_r r = 0$, in the design of an output tracking controller with observer in the continuous-time domain. Spurgeon[10] gives an advanced hyperplane design technique, using a linear equivalent control generated from an appropriately selected hyperplane and it provides superior performance to that obtained using a complex nonlinear control structure. Linear-quadratic-regulator (LQR)-based sliding surface design, which allows one to specify a desired weighting matrix and a desired real eigenvalue, is given by Tang and Misawa.[11]

Currently, robust sliding mode algorithms for discrete systems are being studied by many researchers. These approaches involve switching and nonswitching types of control. Elmali and Olgac[12] and Chan[13] propose nonswitching SM controllers, in which the controller contains an estimate of the perturbations. The controller proposed by Chan is simple and easy to implement, but its disadvantage is that the controller is robust only against slowly varying perturbations. Eun and Cho[14] study the robustness of multivariable DVSC by making use of an uncertainty estimator. Their approach requires a bound on rate of change of the uncertainties to ensure robust stability. Furuta and Pan[15] introduce the concept of sliding sector for SISO regulator-type systems, both continuous-time and discrete-time VSCS. According to them, the sliding sector is a region around the SS, enclosed by two surfaces and inside which a norm of the system state decreases without any control action. A nonswitching-type control law is used to avoid chattering by Cheng et al.[16] for regulator type discrete-time SM MIMO controller design. This controller drives the state trajectories into a bounded region around the origin, in the presence of bounded matched perturbations, but it does not take into account the tracking requirement and mismatched uncertainties. Chen et al.[17] present a boundary-layer approach to reduce chattering in which the width of the boundary layer depends on the state norm for an uncertain linear system.

Missile autopilots are designed to provide stability, performance, and robustness over a wide range of flight conditions. The equations of motion that govern the dynamics of the missile are nonlinear, time varying, and coupled.[18] The optimal time-varying sliding surface is designed by Salamci and Ozgoren,[19] for a missile autopilot by recursively approximating the nonlinear systems as linear time-varying systems. Thukral and Innocenti[20] present VSC design for a missile autopilot that uses both aerodynamic control and reaction jet thrusters to achieve high-angle-of-attack maneuvering. It is well known that the linear time-invariant models developed for design purpose are stable and can deliver satisfactory performance. Bhat et al.[21] use a linearized missile model to design a pitch autopilot by using continuous-time variable structure controller with power rate reaching law to track a given lateral acceleration guidance command of step of magnitude 20 g. A similar work is done for a SISO missile system that uses a dynamic equivalent control combined with sliding mode control to track a unit step input, but the response shows large oscillations, which are undesirable.[22] A robust feed-forward tracking control design using reaching law with DSM controller and its application to an experimental set up of a stage driven by a linear motor is given by Wang et al.[23]

This paper presents a pitch autopilot design for a dual-input air-to-air missile using discrete-time variable structure (DVS) controller with a sliding sector. The missile control problem under consideration is to track the normal acceleration a_z of the pitch plane dynamics. The optimal sliding function σ_k is obtained by minimizing a linear quadratic performance index,[24] which weighs all of the states, control input, tracking error, and also discrete equivalent of the integral tracking error. The sliding sector is designed by considering the dissipativeness property[25] of the system, which means that the system absorbs more energy from the external world than it supplies. The sliding-sector design for DVSC through dissipativeness property is a new approach, which has not been reported in the literature so far. The advantage of using this method is that it deals with the input–output energy; hence, it is a more appropriate condition for a tracking system. The sliding sector is designed so that the system is dissipative inside as well as outside the sector. In this paper, chattering is reduced by a proper design of reaching law and sliding sector.

II. Discrete Variable Structure Tracking Controller

In this section, a discrete variable structure tracking controller with a sliding sector is designed such that a Lyapunov function $V_k = \sigma_k^T \sigma_k$ decreases in the entire state space, that is, both inside and outside the sliding sector. Let the completely controllable and observable discrete-time nominal plant be given by

$$x_{\mathrm{pk}+1} = \Phi_p x_{\mathrm{pk}} + \Gamma_p u_k, \qquad y_{\mathrm{tk}} = C_p x_{\mathrm{pk}} \tag{4}$$

where $x_{\mathrm{pk}} \in \Re^{n_p}$ is the state variable, control input $u_k \in \Re^m$ and $y_{\mathrm{tk}} \in \Re^{n_t}$ is the output to be tracked. Figure 1 shows the discrete variable structure sliding mode controller for tracking the output y_{tk} with respect to the reference input r_k. To enable the system for tracking the output y_{tk} with zero steady-state error, a discrete equivalent of an integrator is added in the outer loop. A unit delay of one sampling time is introduced after the controller, to take into account of the computational delay. Here the controller is coupled because all states and also the tracking error are fedback to all of the inputs, thus getting a larger design freedom so as to achieve a better performance.

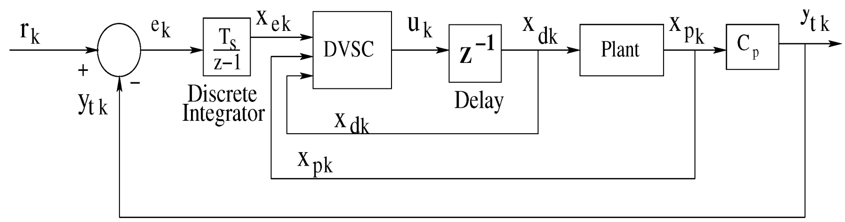

Fig. 1 Block diagram of the DVSC for a tracking system.

In the block diagram, the tracking error $e_k = r_k - y_{\text{tk}}$. The error state x_{ek}, which is the discrete equivalent of an integral of the tracking error e_k and delay states x_{dk}, are given by the difference equation,

$$x_{\text{ek}+1} = x_{\text{ek}} + T_s e_k = x_{\text{ek}} - T_s C_p x_{\text{pk}} + T_s r_k \tag{5}$$

and

$$x_{\text{dk}+1} = u_k$$

where $T_s > 0$ is the sampling period. The plant is augmented with the integrator and delay states to get

$$\begin{bmatrix} x_{\text{ek}+1} \\ x_{\text{pk}+1} \\ \hline x_{\text{dk}+1} \end{bmatrix} = \left[\begin{array}{cc|c} I_{n_t} & -T_s C_p & 0 \\ 0 & \Phi_p & \Gamma_p \\ \hline 0 & 0 & 0 \end{array}\right] \begin{bmatrix} x_{\text{ek}} \\ x_{\text{pk}} \\ \hline x_{\text{dk}} \end{bmatrix}$$

$$+ \begin{bmatrix} 0 \\ 0 \\ \hline I_m \end{bmatrix} u_k + \begin{bmatrix} I_{n_t} \\ 0 \\ \hline 0 \end{bmatrix} T_s r_k \tag{6}$$

where n_t is the number of output to be tracked. Equation (6) can be rewritten with $x_k = [x_{\text{ek}}, x_{\text{pk}}, x_{\text{dk}}]^T \in \Re^n$ as

$$x_{k+1} = \Phi x_k + \Gamma u_k + \Gamma_r r_k \tag{7}$$

$$y_{\text{tk}} = C_t x_k = [C_{t1} \quad C_{t2}] x_k \qquad \text{where} \qquad C_t = [0 \quad C_p \quad 0]$$

The controller design consists of two parts: the switching surface design and the control law design. The switching surface is designed so that the system will have desired characteristics on the SS and the closed-loop system behave as a reduced-order dynamics (ROD) while moving on the SS. In discrete-time domain, there exists a switching region instead of a SS because of the finite sampling time. Hence in this paper, a sliding sector is designed so that the overall system is dissipative with respect to a supply rate. The control law ensures reaching and sliding conditions, and it is shown that a candidate Lyapunov function V_k decreases inside and outside the sector with this control law.

Switching Surface Design

To design the switching surface, the state-space realization of the augmented plant in Eq. (7) is split into regular form as

$$\begin{bmatrix} x_{1k+1} \\ x_{2k+1} \end{bmatrix} = \begin{bmatrix} \Phi_{11} & \Phi_{12} \\ \Phi_{21} & \Phi_{22} \end{bmatrix} \begin{bmatrix} x_{1k} \\ x_{2k} \end{bmatrix} + \begin{bmatrix} 0 \\ \Gamma_2 \end{bmatrix} u_k + \begin{bmatrix} \Gamma_{r_1} \\ 0 \end{bmatrix} r_k$$

The square matrix $\Gamma_2 \in \Re^m$ is nonsingular because the plant input matrix Γ_p is assumed to be of full rank. A reference-command-dependent linear SS of the form

$$\sigma_k = S x_k - S_r r_{k-1} = S_1 x_{1k} + S_2 x_{2k} - S_r r_{k-1}, \qquad \sigma_k \in \Re^m \tag{8}$$

is considered for the tracking controller design. This SS can be considered as a time-varying linear surface as shown in Fig. 2, when the reference command signal is a time-varying arbitrary signal. For simplicity of description, a two-dimensional SS is considered. The slope of the switching function σ_k remains constant, whereas the intercept varies depending on r_{k-1}. When the reference signal is zero (i. e., regulator problem), SS passes through the origin, as seen in the figure. The extreme lines of SS correspond to the maximum value of reference signal $\pm r_{k\,\text{max}}$. In Eq. (8), r_{k-1} term is used instead of r_k to avoid a noncausal feed-forward term r_{k+1} in the linear control.

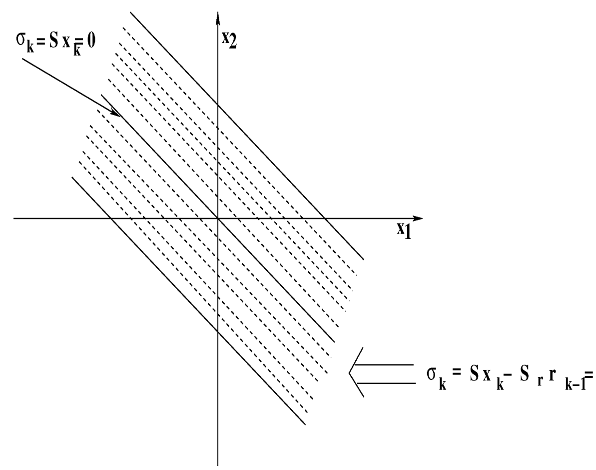

Fig. 2 Reference-command-dependent linear SS, $\sigma_k = Sx_k - S_r r_{k-1}$.

On the switching surface,

$$\sigma_k = 0 \Rightarrow x_{2k} = -S_2^{-1} S_1 x_{1k} + S_2^{-1} S_r r_{k-1} \tag{9}$$

The reduced-order dynamics can be written as

$$x_{1k+1} = \Phi_{11} x_{1k} + \Phi_{12}[F x_{1k} + G r_{k-1}] + \Gamma_{r_1} r_k \tag{10}$$

where

$$F = -S_2^{-1} S_1 \qquad \text{and} \qquad G = S_2^{-1} S_r \tag{11}$$

By defining $\tilde{\Phi} = \Phi_{11}$, $\tilde{\Gamma} = \Phi_{12}$, $\tilde{C}_t = C_{t1}$, $\tilde{x} = x_1$, and $\tilde{D} = C_{t2}$, Eq. (10) becomes

$$\tilde{x}_{k+1} = \tilde{\Phi}\tilde{x}_k + \tilde{\Gamma}\tilde{u}_k + \Gamma_{r_1} r_k \quad \text{where} \quad \tilde{u}_k = F\tilde{x}_k + G r_{k-1} \tag{12}$$

$$y_{\text{tk}} = C_{t1} x_{1k} + C_{t2} x_{2k} = \tilde{C}_t \tilde{x}_k + \tilde{D}\tilde{u}_k$$

F and G are design matrices, and it should be determined such that the reduced-order dynamics is stable and has desired characteristics. Here F acts as feedback gain, and G acts as a feed forward gain. The LQR technique is used to obtain F and G, the derivation of which is given in Appendix. Taking $S_2 = I_m$, S and S_r are obtained as

$$S = [-F \quad I_m] \qquad \text{and} \qquad S_r = G \tag{13}$$

Discrete Sliding-Sector Design

A new, simple, and effective design algorithm for designing the sliding sector is obtained by using the property called dissipativeness, which is characterized by the existence of a function that can be interpreted as an abstract stored energy of the system. Let the supply rate[25] associated with the system given by Eq. (7) be

$$L(x_k, r_k) = x_k^T Q x_k + 2x_k^T N r_k + r_k^T R r_k \tag{14}$$

where $Q \in \Re^{n\times n}$ is a positive-semidefinite symmetric matrix and $R \in \Re^{n_t \times n_t}$ is a positive-definite symmetric matrix. The supply rate is an abstraction of the concept of input power, and in physical systems it is associated with the concept of stored energy. Let the system given by Eq. (7), with a linear control law of the form $u_l = k_1 x_k + k_2 r_k + k_3 r_{k-1}$ be written as

$$x_{k+1} = \Phi_{\text{eq}} x_k + \Gamma_{r\,\text{eq}} r_k + \Gamma_{\text{rd}} r_{k-1} \tag{15}$$

where

$$\Phi_{\text{eq}} = \Phi + \Gamma k_1, \qquad \Gamma_{r\,\text{eq}} = \Gamma k_2 + \Gamma_r \qquad \text{and} \qquad \Gamma_{\text{rd}} = \Gamma k_3$$

where k_1, k_2, and k_3 are derived in the sequel. If the system is dissipative for a reference input r_k, then it will be dissipative with the r_{k-1} input. A necessary and sufficient condition[25] for the system, $x_{k+1} = \Phi_{\text{eq}} x_k + \Gamma_{r\,\text{eq}} r_k$ to be dissipative with respect to supply rate Eq. (14), is that there exists matrices P, M, and W, with P a nonnegative-definite symmetric matrix, satisfying the following equations:

$$\Phi_{\text{eq}}^T P \Phi_{\text{eq}} - P + Q - MM^T = 0, \qquad MW - N - \Phi_{\text{eq}}^T P \Gamma_{r\,\text{eq}} = 0$$

$$R + \Gamma_{r\,\text{eq}}^T P \Gamma_{r\,\text{eq}} - W^T W = 0 \tag{16}$$

The solution of Eq. (16) for the unknown P, M, and W can be obtained from the well-known discrete riccati equation. Rearranging the preceding equations in quadratic form as follows,

$$x_k^T \left(\Phi_{\text{eq}}^T P \Phi_{\text{eq}} - P + Q - MM^T\right) x_k$$

$$+ 2x_k^T \left(MW - N - \Phi_{\text{eq}}^T P \Gamma_{r\,\text{eq}}\right) r_{k-1}$$

$$+ r_{k-1}^T \left(R + \Gamma_{r\,\text{eq}}^T P \Gamma_{r\,\text{eq}} - W^T W\right) r_{k-1} = 0 \tag{17}$$

This expression can be rewritten in terms of the switching function σ_k and sliding-sector parameter δ_k as

$$\sigma_k^T \sigma_k - \delta_k^T \delta_k = \hat{x}_k^T \tilde{N} \hat{x}_k \tag{18}$$

where $\sigma_k^T \sigma_k = \hat{x}_k^T S_d \hat{x}_k$, $\delta_k^T \delta_k = \hat{x}_k^T D \hat{x}_k$, and $\hat{x}_k = [x_k, r_{k-1}]^T$, with the matrices

$$S_d = \begin{bmatrix} Q & -N \\ -N^T & R \end{bmatrix}, \qquad D = \begin{bmatrix} P & 0 \\ 0 & W^T W \end{bmatrix} \tag{19}$$

and

$$\tilde{N} = \begin{bmatrix} MM^T - \Phi_{\text{eq}}^T P \Phi_{\text{eq}} & \Phi_{\text{eq}}^T P \Gamma_{r\,\text{eq}} - MW \\ \left(\Phi_{\text{eq}}^T P \Gamma_{r\,\text{eq}} - MW\right)^T & -\Gamma_{r\,\text{eq}}^T P \Gamma_{r\,\text{eq}} \end{bmatrix}$$

On using the definition of SS, that is, σ_k in Eq. (8), the matrices Q, N, and R are obtained as $Q = S^T S$, $N = S^T S_r$, and $R = S_r^T S_r$. The sliding-sector parameter δ_k is defined so as to satisfy the conditions for the system to be dissipative inside as well as outside the sliding sector. The sliding sector $\mathcal{J}_d$ can now be defined as

$$\mathcal{J}_d = \left\{ x_k \,\middle|\, \sigma_k^T \sigma_k - \delta_k^T \delta_k \le 0, \qquad \forall \quad x_k \in \Re^n \right\}$$

or

$$\mathcal{J}_d = \left\{ x_k | \|\sigma_k\| \le \|\delta_k\|, \qquad \forall \quad x_k \in \Re^n \right\} \tag{20}$$

The width of the sliding sector $\|\delta_k\| = \sqrt{(\hat{x}_k^T D \hat{x}_k)}$ depends on the norm of the system state and the reference input. Hence the sliding sector just defined is a variable-width sliding sector, and it takes into account of the uncertainties and the time-varying reference input. The sliding sector defined in Eq. (20) along with the switching surface $\sigma_k = 0$ is shown in Fig. 3. For simplicity, a two-dimensional space is taken to describe the sliding sector.

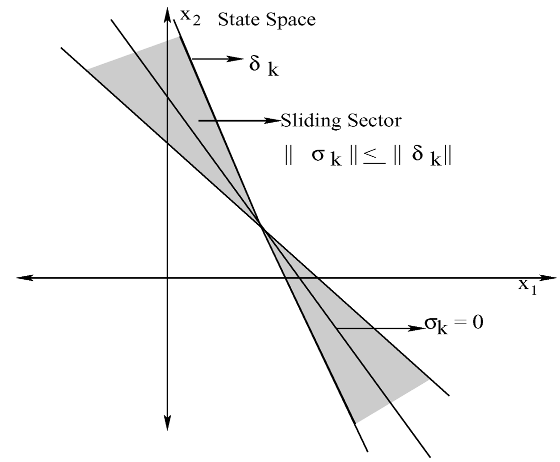

Fig. 3 Sliding function and sliding sector.

Sliding-Sector Design Algorithm

The following steps give a clear idea of the sliding-sector design:

1) Find the switching surface matrices S and S_r as given in Eq. (13) and obtain the SS, σ_k as in Eq. (8).

2) Determine Q, N, and R as $Q = S^T S$, $N = S^T S_r$, and $R = S_r^T S_r$.

3) Solve the set of equations (16) for the unknown P, M, and W.

4) Determine the sliding-sector parameter matrix D by Eq. (19).

5) Obtain $\|\delta_k\| = \sqrt{(\hat{x}_k^T D \hat{x}_k)}$ and the sliding sector as $\|\sigma_k\| \le \|\delta_k\|$ (online computation).

Discrete Variable Structure Control Law

Based on the sliding sector just given, a DVS controller is designed such that 1) a candidate Lyapunov function V_k defined as $V_k = \sigma_k^T \sigma_k$ keeps decreasing both inside and outside of the sliding sector, 2) the system state is moved from the outside to the inside of the sliding sector, and 3) the system state is constrained to stay inside the sliding sector without chattering. The DVS controller designed by Furuta and Pan[15] does not ensure 3), as there is no control input inside the sliding sector. In this paper, the DVS control law is designed to move the system state from the outside to the inside of the sliding sector with $u_k = u_0$, $\forall\, x_k \bar{\in} \mathcal{J}_d$ and subsequently, use control $u_k = u_l$, $\forall\, x_k \in \mathcal{J}_d$ to keep it within the sector, once it enters the sector. The u_0 is in the form of $u_l + u_d$, where u_l is the linear part and u_d is the discontinuous part of the control law, and u_l is derived so as to satisfy the relation $\sigma_{k+1} - \beta\sigma_k = 0$ as

$$u_l = -(S\Gamma)^{-1}[(S\Phi - \beta S)x_k + (S\Gamma_r - S_r)r_k + \beta S_r r_{k-1}]$$

$$u_l = k_1 x_k + k_2 r_k + k_3 r_{k-1} \tag{21}$$

where

$$k_1 = -(S\Gamma)^{-1}(S\Phi - \beta S), \qquad k_2 = -(S\Gamma)^{-1}(S\Gamma_r - S_r)$$

and

$$k_3 = -(S\Gamma)^{-1}\beta S_r$$

The design parameter β is a diagonal matrix satisfying $0 \le \beta_i \le 1$, for $i = 1 : m$.

Theorem: For any controllable discrete-time plant described by Eq. (7), the DVS control law

$$u_k = \begin{cases} u_l, & \forall \quad x_k \in \mathcal{J}_d \\ u_0 = u_l + u_d, \qquad \text{where} \qquad u_d = -(S\Gamma)^{-1} k_d Sgn(\sigma_k)\|\delta_k\|, & \forall \quad x_k \bar{\in} \mathcal{J}_d \end{cases} \tag{22}$$

makes the system asymptotically stable, if $S\Gamma$ is invertible and $\beta_n + k_{\mathrm{dn}} \leq 1$, where k_d is a diagonal matrix, $k_{\mathrm{dn}} = \|k_d Sgn(\sigma_k)\|$ and $\beta_n = Sup\{\beta_i\}$. The u_l and u_0 are the control inputs inside and outside the sliding sector, respectively, and are designed so that the Lyapunov function $V_k = \sigma_k^T \sigma_k$ decreases both inside and outside the sliding sector. □

Proof:

Case 1 : For $x_k \in \mathcal{J}_d$, $u_k = u_l$, and the closed-loop system is given by

$$x_{k+1} = \Phi x_k + \Gamma u_k + \Gamma_r r_k = \Phi_{\mathrm{eq}} x_k + \Gamma_{r\,\mathrm{eq}} r_k + \Gamma_{\mathrm{rd}} r_{k-1} \quad (23)$$

The Lyapunov function $V_k = \sigma_k^T \sigma_k$ decreases inside the sector because $\sigma_{k+1} - \beta\sigma_k = 0$, which implies satisfaction of the discrete sliding condition $\|\sigma_{k+1}\| \leq \|\sigma_k\|$. Hence,

$$\Delta V_k = V_{k+1} - V_k = \sigma_{k+1}^T \sigma_{k+1} - \sigma_k^T \sigma_k \leq 0$$

Case 2 : Outside the sliding sector, $x_k \bar{\in} \mathcal{J}_d$, the control law $u_k = u_0$, and $\|\delta_k\| < \|\sigma_k\|$.
Here

$$\sigma_{k+1} = \beta\sigma_k - k_d Sgn(\sigma_k)\|\delta_k\|$$

$$\text{where} \qquad Sgn(\sigma_k) = \begin{bmatrix} sgn(\sigma_{1k}) \\ : \\ sgn(\sigma_{mk}) \end{bmatrix}$$

$$\begin{aligned} \|\sigma_{k+1}\| &\leq \beta_n\|\sigma_k\| + \|k_d Sgn(\sigma_k)\|\|\delta_k\| \\ &\leq [\beta_n + k_{\mathrm{dn}}]\|\sigma_k\| \\ &\leq \|\sigma_k\|, \qquad \text{if} \qquad \beta_n + k_{\mathrm{dn}} \leq 1 \end{aligned}$$

Hence $V_{k+1} \leq V_k$ or $\Delta V_k < 0$. Thus the Lyapunpov function decreases outside the sliding sector ensuring reaching of the sliding sector. Hence it has been shown that the Lyapunov function V_k keeps on decreasing in the entire state space with the DVS control law Eq. (22), which provides an asymptotically stable discrete-time control system. It has been proved[16] that the (n-m) eigenvalues of the closed-loop system given by Eq. (23) are determined by the reduced-order system

$$x_{k+1} = [\Phi - \Gamma(S\Gamma)^{-1}S\Phi]x_k \quad (24)$$

$$\sigma_k = Sx_k = 0 \quad (25)$$

and the rest m eigenvalues are given by β_i. To study the robust performance of this controller [Eq. (22)], the system in the presence of uncertainties is considered next.

III. System with Additive Uncertainties

Let the perturbed plant with both matched and mismatched additive uncertainties be given by

$$x_{k+1} = (\Phi + \Delta\Phi)x_k + \Gamma u_k + \Gamma_r r_k + f(x, k, u) \quad (26)$$

where $\Delta\Phi$ is the mismatched parameter uncertainty in the plant matrix Φ, norm bounded by an unknown positive scalar h and $f(x, k, u)$ is the lumped matched uncertainty, which can be represented as

$$\|\Delta\Phi\| \leq h \quad (27)$$

$$f(x, k, u) = \Gamma v(x, k, u), \qquad \|v(x, k, u)\| \leq \rho \quad (28)$$

Here $v(x, k, u)$ can be comprised of uncertainties, nonlinearities of the system, and external disturbances. It is assumed that the norm of the matched uncertainty is bounded by an unknown positive constant ρ, as given in Eq. (28). For simplicity $v(x, k, u)$ is written as v_k. Without loss of generality, any uncertainty present in the input distribution matrix Γ is assumed to be incorporated in the system disturbance term $f(x, k, u)$. The DVS control law given in Eq. (22) ensures the system state to move from outside to inside of the sliding sector and finally to bring the trajectories into the vicinity of the SS, even in the presence of matched and mismatched bounded uncertainties.

Case 1: Inside the sliding sector, $\|\sigma_k\| \leq \|\delta_k\|$, and $u_k = u_l$.

$$\sigma_{k+1} = \beta\sigma_k + S\Delta\Phi x_k + S\Gamma v_k \quad (29)$$

$$\begin{aligned} \|\sigma_{k+1}\| &\leq \|\beta\sigma_k\| + \|S\Delta\Phi x_k\| + \|S\Gamma v_k\| \\ &\leq [\beta_n + h_\Phi + \rho_m]\|\sigma_k\| \\ \|\sigma_{k+1}\| &\leq \|\sigma_k\| \qquad \text{if} \qquad \beta_n + h_\Phi + \rho_m \leq 1 \end{aligned} \quad (30)$$

where

$$\beta_n = Sup\{\beta_i\}, \qquad h_\Phi = \|S\Delta\Phi x_k\|/\|\sigma_k\|$$
$$\text{and} \qquad \rho_m = \|S\Gamma v_k\|/\|\sigma_k\| \quad (31)$$

Hence the state trajectories will be driven towards the SS and remain in the close neighborhood of $\sigma_k = 0$ when the uncertainties satisfies the norm condition.

Case 2: Outside the sliding sector,

$$\sigma_{k+1} = S\Delta\Phi x_k + S\Gamma v_k + \beta\sigma_k - k_d sgn(\sigma_k)\|\delta_k\| \quad (32)$$

$$\begin{aligned} \|\sigma_{k+1}\| &\leq \|S\Delta\Phi x_k\| + \|S\Gamma v_k\| + \beta_n\|\sigma_k\| + k_{\mathrm{dn}}\|\delta_k\| \\ &\leq [h_\Phi + \rho_m + k_{\mathrm{dn}} + \beta_n]\|\sigma_k\| \\ &\leq \|\sigma_k\|, \qquad \text{if} \qquad h_\Phi + \rho_m + k_{\mathrm{dn}} + \beta_n \leq 1 \end{aligned} \quad (33)$$

The diagonal elements of k_d and β are selected so that Eq. (33) is satisfied. The conditions given by Eq. (30) and Eq. (33) are sufficient conditions, which are highly conservative; hence, to obtain bound on $\Delta\Phi$ and v_k, scaling factors $h_r \leq 1$ and $\rho_r \leq 1$ are taken such that

$$\|S\Delta\Phi x_k\| \leq h_r\|S\|\|\Delta\Phi\|\|x_k\| \quad \text{and} \quad \|S\Gamma v_k\| \leq \rho_r\|S\|\|\Gamma\|\|v_k\|$$

Now the bound on the matched and mismatched uncertainties can be written as

$$\|v_k\| \leq \rho, \qquad \rho < \frac{\eta(1 - \beta_d)\|\sigma_k\|}{\|S\|\|\Gamma\|\rho_r} \quad (34)$$

$$\|\Delta\Phi\| \leq h, \qquad h < \frac{(1 - \eta)(1 - \beta_d)\|\sigma_k\|}{\|S\|\|x_k\|h_r} \quad (35)$$

where $\beta_d = \beta_n + k_{\mathrm{dn}}$ and η is such that $0 \leq \eta \leq 1$. The switching function σ_k will keep on decreasing if the preceding sufficient conditions are satisfied. However for a particular value of β_n and uncertainties $\Delta\Phi$ and v_k, σ_k will be a small, nonzero value, and it can be obtained from Eq. (30) as

$$\|\sigma_k\| \geq \frac{\|S\Delta\Phi x_k\| + \|S\Gamma v_k\|}{1 - \beta_n} \quad (36)$$

Equation (36) gives the least upper bound on $\|\sigma_k\|$, and if it satisfies $\|\sigma_k\| \leq \|\delta_k\|$ then the DVS controller works satisfactorily. Thus from Eq. (33), $\|\sigma_{k+1}\| \leq \|\sigma_k\| \Rightarrow \Delta V_k \leq 0$. This shows that the Lyapunov's stability criteria is satisfied both inside and outside the sliding sector with the DVS control law, hence providing an asymptotically stable system in the presence of additive uncertainties.

IV. DVSC Applied to Missile Tracking

The missile dynamics is highly uncertain because of large variations in dynamic pressure and in precise knowledge of aerodynamic coefficients and is also subjected to large external disturbances. Hence it needs a robust control approach like VSC for the controller design. A dual-input air-to-air missile with cruciform wings is considered here, and the short-period dynamics of the missile are used for the design of controller. The linearized equations of motion of the missile in pitch plane are given by

$$\dot{\alpha} = (Z_\alpha/V)\alpha + q + \left(Z_{\delta_w}/V\right)\delta_w + \left(Z_{\delta_t}/V\right)\delta_t$$
$$\dot{q} = M_\alpha\alpha + M_q q + M_{\delta_w}\delta_w + M_{\delta_t}\delta_t \tag{37}$$

where α is the angle of attack (AOA) in rad, q is the pitch rate in rad/second, and V is the missile forward velocity in meters/second. The wing and tail control surface deflections in rad are δ_w and δ_t respectively, and Z_α, M_α, Z_δ, M_q, etc. are the aerodynamic stability derivatives. The missile is assumed to have the following wing and tail actuator dynamics as

$$\tau_w\dot{\delta}_w + \delta_w = \delta_{\mathrm{wc}}, \qquad \tau_t\dot{\delta}_t + \delta_t = \delta_{\mathrm{tc}} \tag{38}$$

where τ_w and τ_t are the actuator time constants and δ_{wc}, δ_{tc} are the wing and tail actuator commands in rad. The output for tracking the LATAX command r_k is the measured acceleration a_z given by

$$a_z = V(\dot{\alpha} - q) + l\dot{q}$$

hence

$$a_z = (Z_\alpha + lM_\alpha)\alpha + lM_q q + \left(Z_{\delta_w} + lM_{\delta_w}\right)\delta_w + \left(Z_{\delta_t} + lM_{\delta_t}\right)\delta_t \tag{39}$$

where l is the distance of the accelerometer ahead of center of gravity. After augmentation of the actuator states, let the state-space model of the plant in continuous-time domain be written as

$$\dot{x}_p = A_p x_p + B_p u, \qquad y_t = C_p x_p \tag{40}$$

The discretized state-space model and the tracking output can be written as in Eq. (4), with plant states $x_{\mathrm{pk}} = [\alpha, q, \delta_w, \delta_t]^T$ and input $u_k = [\delta_{\mathrm{wc}}, \delta_{\mathrm{tc}}]^T$. In this paper, the autopilot is designed to meet the following specifications even in the presence of (bounded) parameter uncertainties and external disturbances.

Performance Specifications

Considering the guidance command profile and hardware limitations, the controller specifications and constraints are chosen as follows:

1) The system response specifications are a) settling time ≤ 0.2 s, b) percentage overshoot $\le 5\%$ final value, and c) AOA ≤ 8 deg.

2) The actuator constraints are the maximum permissible deflection of wing and tail control surfaces $\delta_w, \delta_t = \pm 20$ deg and the maximum slew rates $\dot{\delta}_w, \dot{\delta}_t = \pm 300$ deg/s.

V. Simulation Results

Figure 4 shows the discrete variable structure sliding mode controller for tracking the lateral acceleration a_z with respect to the reference input r_k. Here the wing and tail actuators are used to control the missile lateral acceleration. In this figure, x_{ak} represents $[x_{\mathrm{pk}}, x_{\mathrm{dk}}]'$.

Simulation studies are carried out for the linear model of an air-to-air missile at operating condition corresponding to Mach number $M = 4$ by using the software packages MATLAB® and SIMULINK. The main objective of the simulation is to validate the autopilot performance and the efficiency. At the operating point $M = 4$, trim $\alpha = 2.5$ deg, and at $t = 5$ s the plant matrices in continuous-time domain as in Eq. (40) are given next:

$$A_p = \begin{bmatrix} -0.8392 & 1 & -0.4453 & -0.1113 \\ -116.6676 & -0.9445 & 52.6213 & -335.3318 \\ 0 & 0 & -64 & 0 \\ 0 & 0 & 0 & -100 \end{bmatrix}$$

$$B_p = \begin{bmatrix} 0 & 0 \\ 0 & 0 \\ 64 & 0 \\ 0 & 100 \end{bmatrix}$$

and

$$C_p = [-1166.1 \quad -0.5 \quad -561.5 \quad -314.6]$$

A sampling period of 10 ms is used to discretize the plant. For designing the controller, a first-order actuator model is used while simulation is carried out using a second-order actuator model. The robust control objective for this system is to track a lateral acceleration guidance command given by the guidance station, in the presence of uncertainties. Here in the simulation study, two types of reference inputs are considered as 1) guidance command of step input of magnitude 20 g and 2) a typical time-varying LATAX profile. In the controller design, the discretized plant is augmented with the error state and delay states, where the delay states are included to take into account of the computational delay. In the computation of F and G, the weighting matrices Q_1, Q_2, and R_c as in Eq. (A2), in continuous-time domain are selected as

$$Q_1 = diag([0.21, 0, 0, 0, 0]), \qquad Q_2 = 3 \times 10^{-4}$$

$$\text{and} \qquad R_c = \begin{bmatrix} 100 & 0 \\ 0 & 10 \end{bmatrix}$$

Then Q_c is calculated by Eq. (A3), and the discretized weighting matrices are obtained by Eq. (A4). By using Eq. (A8), the optimal feedback gain F and feed-forward gain G are computed and hence the optimal SS σ_k. From $S = [-F \quad I_m]$ and $S_r = G$, the S and S_r matrices are obtained as

$$S = \begin{bmatrix} 0.0368 & 2.9614 & 0.0948 & 0.6053 & -0.1501 & 1 & 0 \\ -0.0032 & -1.415 & -0.1831 & -0.1717 & 1.0164 & 0 & 1 \end{bmatrix}$$

$$S_r = 10^{-4} \times \begin{bmatrix} -0.8549 \\ 0.1001 \end{bmatrix}$$

The eigenvalues of the reduced-order system, when the state trajectory is sliding on the SS, are given by {0.1646,

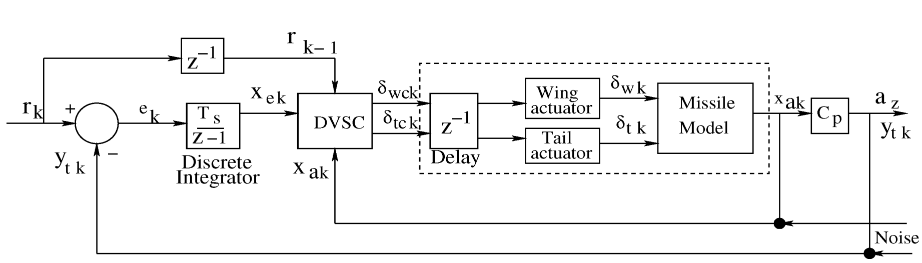

Fig. 4 Block diagram of the DVSC for missile tracking system.

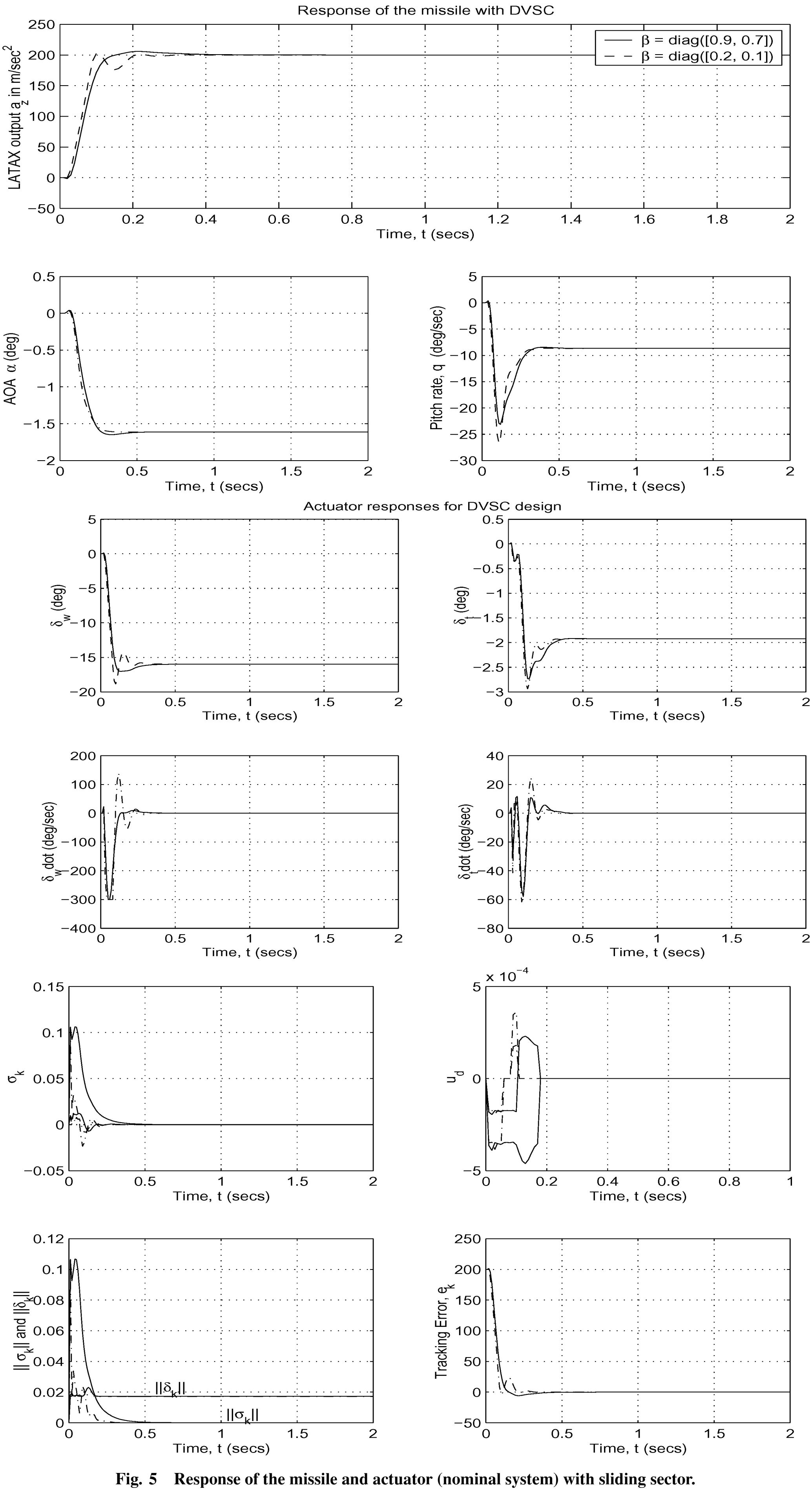

Fig. 5 Response of the missile and actuator (nominal system) with sliding sector.

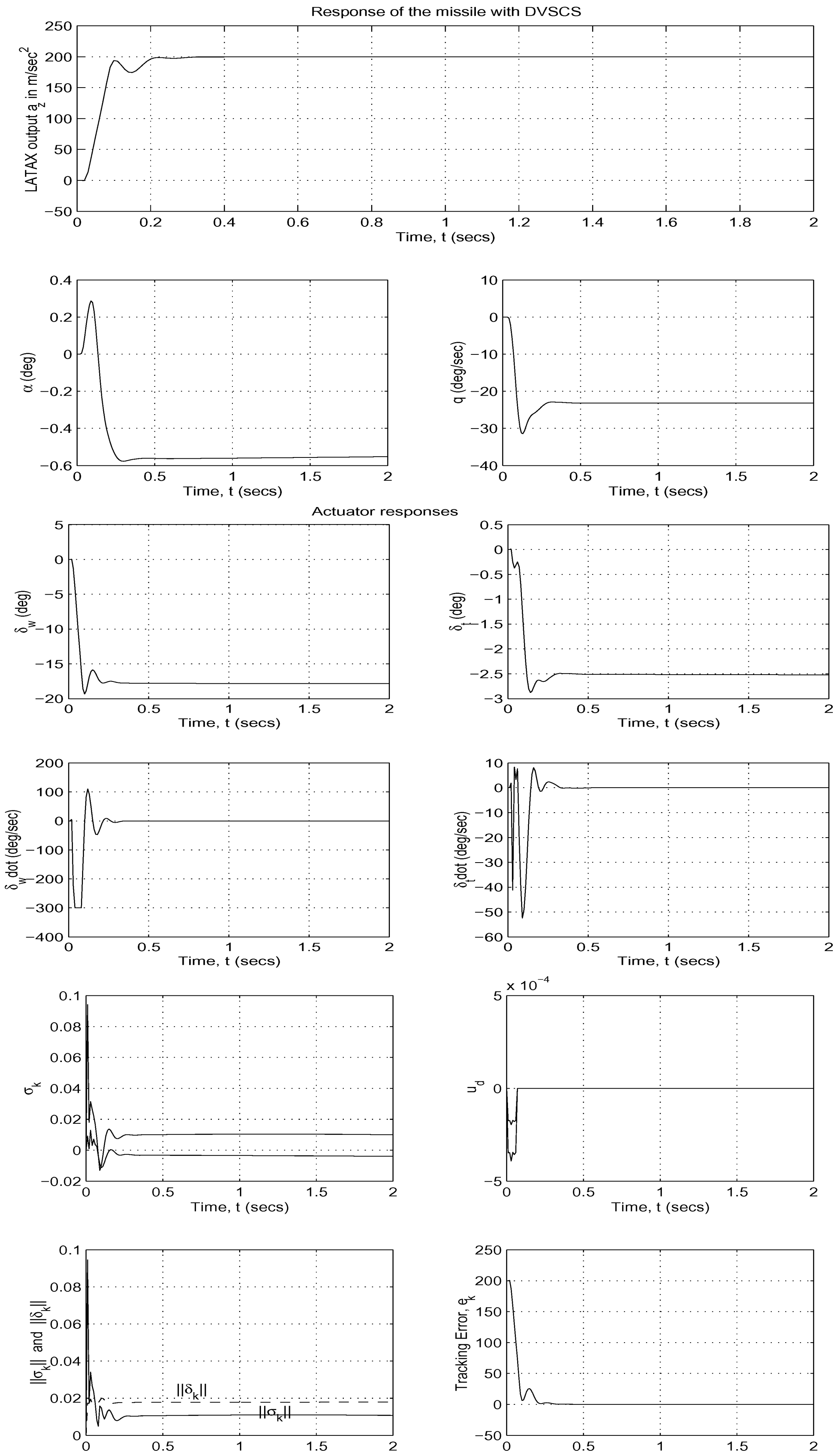

Fig. 6 Response of the missile and actuator with DVSC in the presence of matched and mismatched uncertainties.

0.4924, 0.7446 + 0.0998i, 0.7446 − 0.0998i, 0.7911}. The solution of Eq. (16) for P, M, and W can be obtained as

$$P = \begin{bmatrix} 0.0000 & 0.0020 & 0.0002 & -0.0001 & -0.0011 & 0.0001 & -0.0011 \\ 0.0020 & 3.1061 & 0.3417 & -0.1756 & -1.8187 & 0.2086 & -1.7585 \\ 0.0002 & 0.3417 & 0.0376 & -0.0194 & -0.2002 & 0.0229 & -0.1936 \\ -0.0001 & -0.1756 & -0.0194 & 0.0101 & 0.1032 & -0.0116 & 0.0998 \\ -0.0011 & -1.8187 & -0.2002 & 0.1032 & 1.0657 & -0.1218 & 1.0305 \\ 0.0001 & 0.2086 & 0.0229 & -0.0116 & -0.1218 & 0.0142 & -0.1177 \\ -0.0011 & -1.7585 & -0.1936 & 0.0998 & 1.0305 & -0.1177 & 0.9965 \end{bmatrix}$$

$$M = [-0.0369, -2.7768, -0.0729, -0.6211, 0.0310, -0.9931, -0.1161]^T$$

and

$$W = 8.6088 \times 10^{-5}$$

The matrix D in the sliding-sector definition is determined by Eq. (19), and the sliding sector is obtained as in Eq. (20). The design parameter k_d in the control law Eq. (22) is selected as $diag([0.4, 0.2])$. With $\beta = diag([0.2, 0.1])$, the eigenvalues of Φ_{eq} in Eq. (23) are obtained as {{0.1646, 0.4924 0.7446 ± 0.0998i, 0.7911, 0.2, 0.1}.

The simulation results of the nominal system with DVS control law Eq. (22) are given in Fig. 5. The dotted and solid lines are the responses corresponding to $\beta = diag([0.2, 0.1])$ and

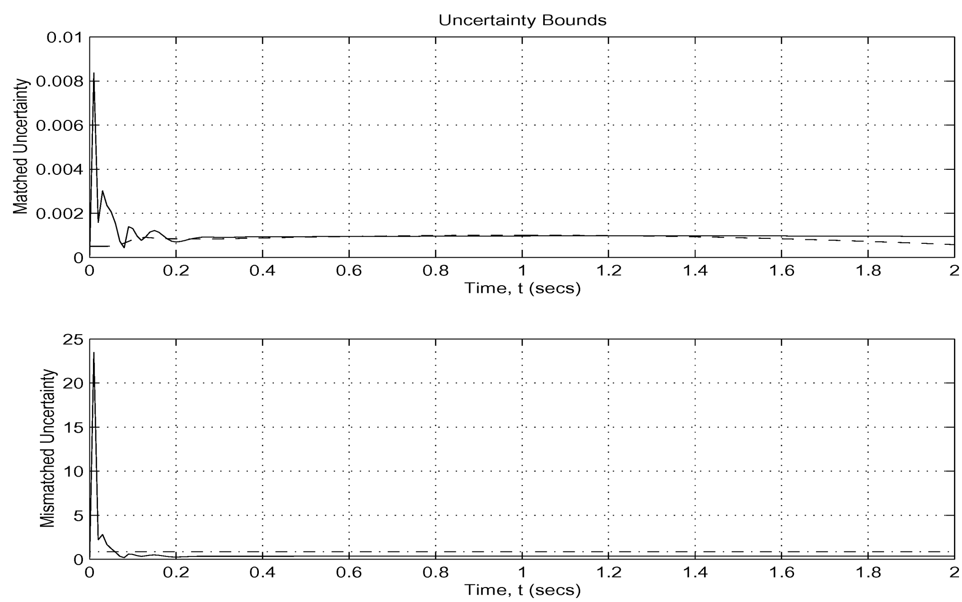

Fig. 7 Uncertainty bounds for $\Delta\Phi$ and v_k.

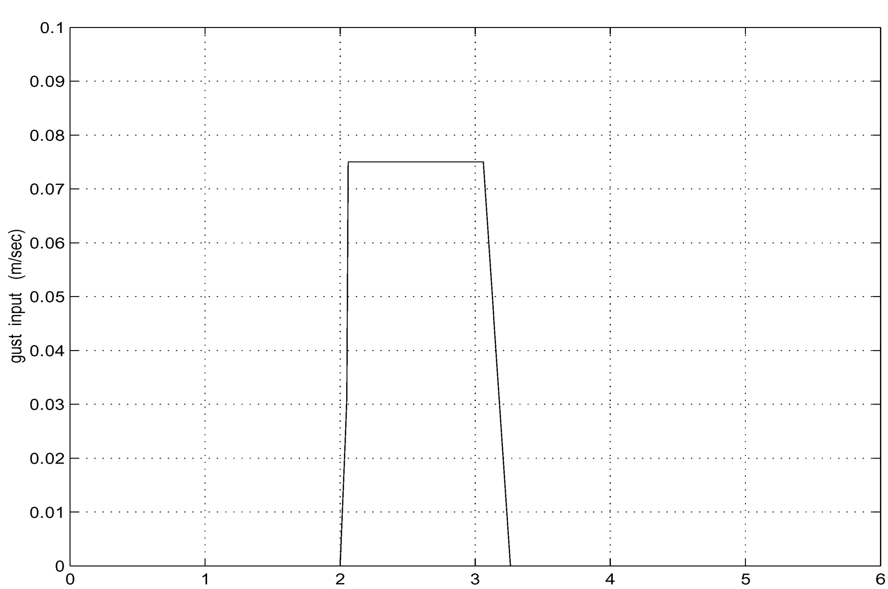

Fig. 8 Wind gust input used in the simulation.

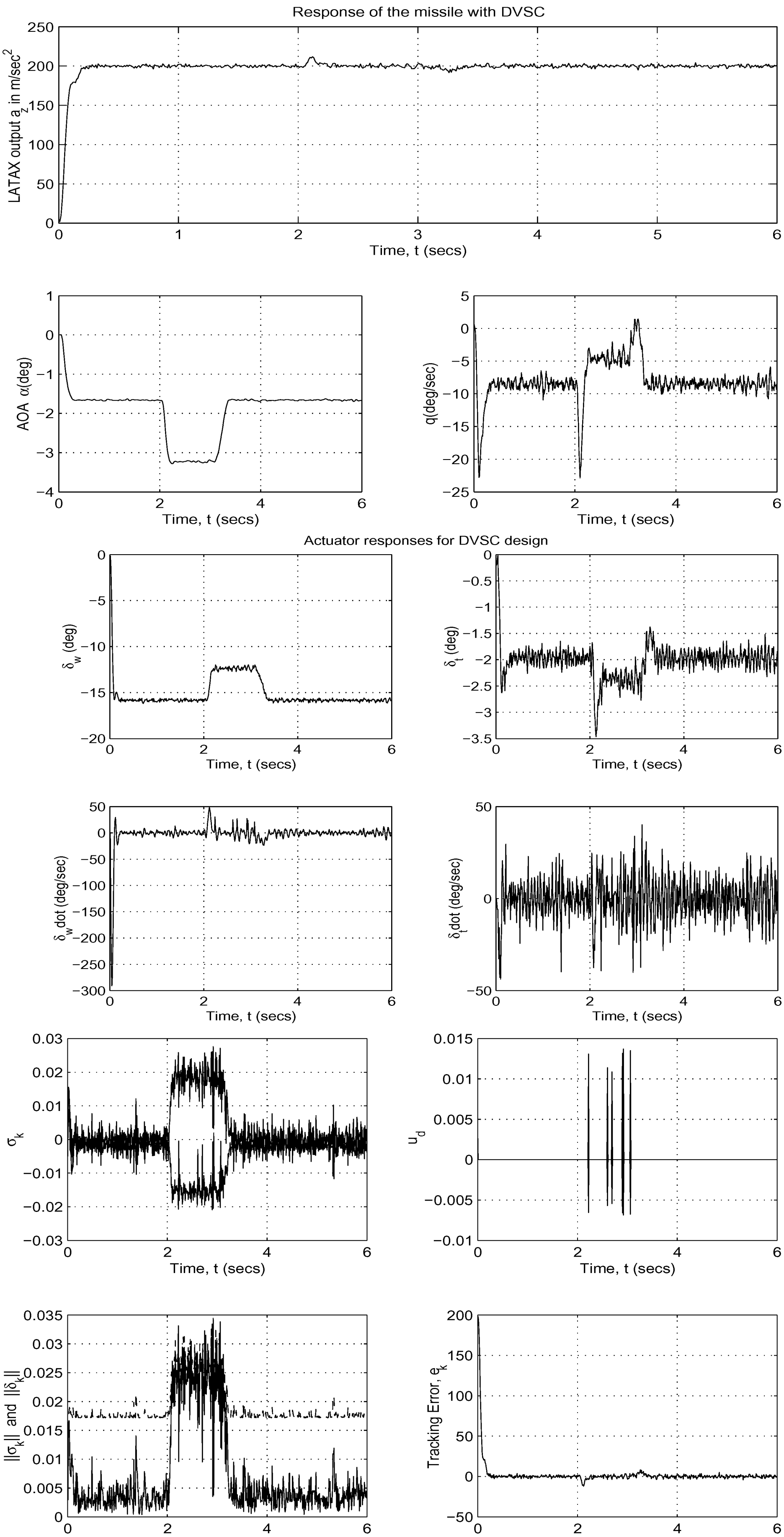

Fig. 9 Response of the missile and actuator with DVS control law in the presence of noise and gust input.

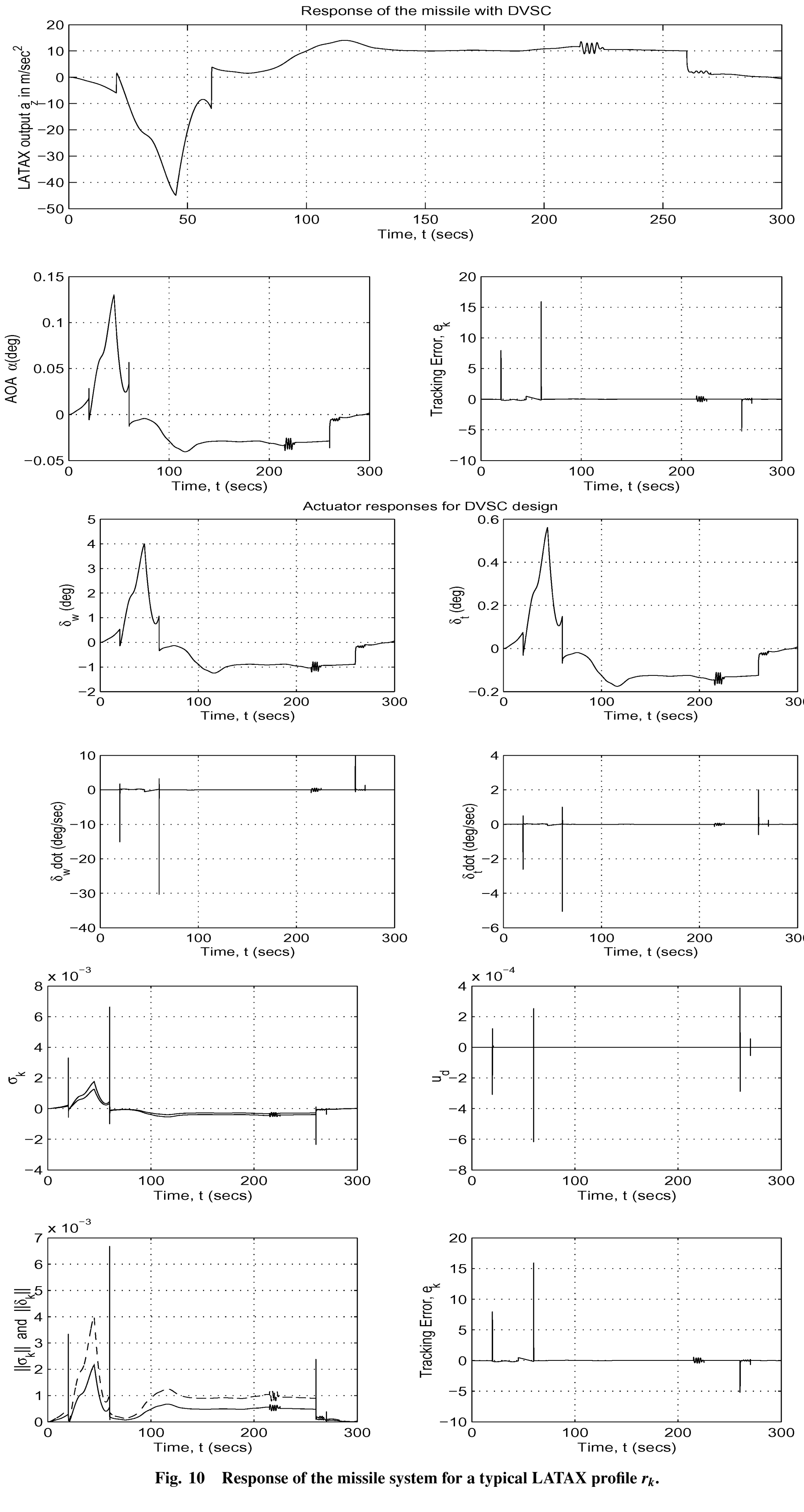

Fig. 10 Response of the missile system for a typical LATAX profile r_k.

$\beta = diag([0.9, 0.7])$, respectively. It is observed that with very small value of β slight oscillations are present in the response plots, but the reaching time and rise time are small. With this DVS controller, perfect tracking is achieved, with a low AOA of -1.64 deg. The wing and tail control surface deflections are -15.9 deg and -1.9 deg, respectively. The wing actuator contributes a major part in generating the lateral acceleration of 200 m/s^2, since the wing control surface is larger than the tail control surface. To limit the actuator rates to ± 300 deg/s, a saturation block is included in the simulation. Actuator saturation might not take place in a practical scenario where the magnitude of the command signal is much smaller than 20 g. The actuator slew rates go to zero approximately in 0.2 s. This controller enables tracking of a LATAX step command of magnitude as high as 20 g with a small rise time of 0.07 s and a settling time of 0.114 s as seen from the a_z vs t response plot. Hence this controller is better suited in a missile application, that is, in the terminal phase of the missile guidance when the missile is closing on to the target. When there is no uncertainty present in the system, the switching function σ_k goes to zero. The nonzero value of u_d indicates the reaching mode. It is observed that within a few sampling instants the state trajectories enter into the sliding sector and thereafter remain inside it. From the plot of u_d, the reaching time is 0.11 s for $\beta = diag([0.2, 0.1])$ and 0.18 s for $\beta = diag([0.9, 0.7])$, and the tracking error goes to zero in 0.3 s. Even though S_r is very small, it is quite acceptable, because the dc gain of the plant is very high for the acceleration output and the system works satisfactorily even if S_r is made zero.

The nominal plant is considered to be the missile model operating at $M = 4$, and the uncertain plant is selected as the missile model at $M = 1.2$. The difference in the system matrices in the continuous-time domain at two operating points is taken as the mismatched plant uncertainty ΔA_p and is given as

$$\Delta A_p = \begin{bmatrix} -0.7086 & 0 & -0.7634 & -0.1909 \\ -59.3288 & -1.5527 & -5.7817 & 65.6204 \\ 0 & 0 & 0 & 0 \\ 0 & 0 & 0 & 0 \end{bmatrix}$$

$\Delta\phi$ in Eq. (26) is the discretized version of ΔA_p. The matched uncertainty[15] $f(k) = \Gamma v_k$ is taken as a nonlinear function in $\alpha, q, \delta_w, \delta_t$ and sampling instant k. Let $v(k) = 0.001[v_1(k), v_2(k)]^T$, where

$$v_1(k) = \alpha^2 - q^2 + \alpha\delta_w - q\cos(k) + \sin(k)$$

$$v_2(k) = \alpha^2 + q^2 + \alpha\delta_w + q\delta_t + 0.5\cos(k)$$

Figure 6 shows the missile responses in the presence of matched and mismatched uncertainties. There is a tradeoff between the design parameters β and k_d with uncertainties; a small value of β is desired to accommodate large uncertainties. Hence $\beta = diag([0.2, 0.1])$ is used in this and later simulations. The controller works efficiently satisfying all of the performance specifications, with a slight increase in settling time to 0.2 s and with the same rise time as for the nominal system. The wing and tail control surface deflections are increased to -18 and -2.5 deg, respectively. The steady-state value of AOA is -0.55 deg and gives a fast response satisfying all other specifications, even in the presence of uncertainties. The reaching time is 0.18 s, and the tracking error goes to zero in 0.4 s. The value of σ_k is not necessarily zero in the presence of uncertainties as in Eq. (36), but it satisfies the condition $\|\sigma_{k+1}\| \le \|\sigma_k\|$. The uncertainty bounds for v_k and $\Delta\Phi$ are given in Fig. 7, which are only a sufficient condition. The dotted lines represent $\|v_k\|$ and $\|\Delta\Phi\|$, and solid lines represent ρ and h . The plot of $\|v_k\|$ satisfies Eq. (34), whereas a plot of $\|\Delta\Phi\|$ does not satisfy Eq. (35). This shows that the system can still give satisfactory responses for higher values of uncertainties for which the norm-bound conditions, Eqs. (34) and (35), might not be fully satisfied. The value of h_r and ρ_r is taken as $h_r = 0.0004$ and $\rho_r = 1$.

Figure 8 gives the plot of the wind gust input of speed 30 m/s, which is equivalent to wind induced in the AOA α, for a duration of 1 s. The response curves for the missile with this wind gust and also with state and measurement noise are shown in Fig. 9. The rise time and settling time are still small, 0.123 and 0.187 s, respectively. The AOA is increased from -1.6 to -3.25 deg, and δ_w and δ_t are well within the limits. The σ_k value is close to zero, and the u_d plot shows that switching occurs during the gust period. The controller tracks the LATAX command even in the presence of noise and gust input with a small tracking error. This controller exhibits a very good disturbance rejection and also shown to be very robust against parameter variations as seen from Figs. 6 and 9.

The simulation results of the system to track a typical LATAX profile generated by a proportional navigation guidance scheme for an air-to-air missile for an incoming target is given in Fig. 10. The LATAX command is for a period of 300 s, and the initial negative g is for the clearing of the launching aircraft and then for the climbing of the missile. Both the the wing and tail control surfaces are active and contribute to generate the required g. As seen from the u_d plot, switching of the controller takes place when r_k varies rapidly. Throughout the control period perfect tracking is achieved, and the σ_k values are close to zero. The difference between the command and the actual measured acceleration is negligibly small, which can also be seen from the bottom plot of Fig. 10 for the tracking error e_k. The tracking error momentarily exists, whenever r_k changes rapidly.

The main advantage with this DVS controller is that for the implementation the upper bound on the matched and mismatched uncertainties, ρ and h need not be known beforehand; instead only the norm-bound conditions are required to be satisfied. This is only a sufficient condition, which is slightly restrictive. The system could still work in stable mode even if $\|v_k\| > \rho$ or $\Delta\phi > h$.

VI. Conclusion

In this paper a missile pitch autopilot is designed using discrete variable structure controller with sliding sector for a dual-input missile to track a given lateral acceleration command of 20 g. A new approach based on the dissipativeness property of the system is used for the variable width sliding-sector design. The optimal switching surface is designed by the linear-quadratic-regulator method so that the ROD will have the desired characteristics. The discrete-time variable structure control law drives the state trajectories into the sliding sector and is constrained to stay inside it thereafter, in the presence of bounded matched and mismatched uncertainties. This controller gives satisfactory performance and very fast tracking with a small angle of attack, and the tracking error goes to zero approximately in 0.12 s. The simulation study with matched and mismatched uncertainties, noise, and gust input indicates that the controller is robust with respect to parameter variations and external disturbances.

Appendix: Optimal SS Design by LQR

F and G are determined so that the reduced-order system Eq. (12) is stable and has the desired characteristics. For the sake of simplicity, the symbol ~ in Eq. (12) is omitted for brevity in the following derivations. Let the performance index (PI) to be minimized for the continuous plant be

$$J_c = \int_0^\infty \left(x^T Q_c x + u^T R_c u\right) \mathrm{d}t \tag{A1}$$

In the SS design, the PI is modified to include the cost term with tracking error without creating confliction, which provides better handle on the response of the system. Hence the generalized PI[24] is of the form

$$J_c = \int_0^\infty \left(u^T R_c u + \bar{y}^T Q_1 \bar{y} + e^T Q_2 e\right) \mathrm{d}t \tag{A2}$$

where Q_1, Q_2 are nonnegative definite symmetric matrices, and e_k is the tracking error. The pseudo output $\bar{y}$ is given by $\bar{y} = \bar{C}x$, $\bar{C} = I - LC_t$, $L = C_t^T(C_t C_t^T)^{-1}$. This PI can be written in convenient form as

$$J_c = \int_0^\infty \left[(x - \bar{x})^T Q_c (x - \bar{x}) + u^T R_c u\right] \mathrm{d}t, \qquad \bar{x} = Lr$$

where

$$Q_c = \bar{C}^T Q_1 \bar{C} + C_t^T Q_2 C_t \tag{A3}$$

To design the controller in the discrete-time domain, it is appropriate to proceed with approximate discretized PI[26]

$$J_d = \frac{1}{2}\sum_{k=0}^{N}(x_k - \bar{x}_k)^T Q_d (x_k - \bar{x}_k) + 2(x_k - \bar{x}_k)^T N_d u_k + u_k^T R_d u_k$$

where

$$Q_d = (T_s/2)\left(\Phi^T Q_c \Phi + Q_c\right), \qquad N_d = (T_s/2)\left(\Phi^T Q_c \Gamma\right) \tag{A4}$$

and

$$R_d = (T_s/2)\left(\Gamma^T Q_c \Gamma\right) + T_s R_c$$

$\bar{x}_k = L r_k$ is some special trajectory, called desired state trajectory, related to the desired output trajectory r_k. By selecting appropriate Q_1, Q_2, and R_c, we can obtain the matrix F and hence S. In practice it is easy to select Q_c and R_c, then use Eq. (44) obtain its discrete version to calculate the feedback gain. Also this takes into account the sampling rate effects on the switching surface design. Now adjoining the state equation with the preceding PI by use of Lagrange multipliers and minimizing with respect to λ_{k+1}, u_k and x_k, give the state equation, costate equation, and the control equation. Based on the sweep method, where $\lambda_k \triangleq P_k x_k + s_k$, one gets the optimal control u_k and the difference equations in P_k and s_k as

$$u_k = -\bar{R}_d^{-1}\left[\left(\Gamma^T P_{k+1}\Phi + N_d^T\right)x_k + \Gamma^T s_{k+1} - N_d^T L r_k\right] \tag{A5}$$

$$P_k = \Phi^T P_{k+1}\Phi - \left(\Gamma^T P_{k+1}\Phi + N_d\right)^T \bar{R}_d^{-1}\left(\Gamma^T P_{k+1}\Phi + N_d\right) + Q_d \tag{A6}$$

$$s_k = \left[\Phi^T - \left(\Phi^T P_{k+1}\Gamma + N_d\right)\bar{R}_d^{-1}\Gamma^T\right]s_{k+1} - Q_r r_k \tag{A7}$$

where

$$\bar{R}_d = \left(R_d + \Gamma^T P_{k+1}\Gamma\right)$$

and

$$Q_r = Q_d L - \left(\Phi^T P_{k+1}\Gamma + N_d\right)\bar{R}_d^{-1} N_d^T L$$

P_k and s_k are the solutions of the preceding backward difference equations. At steady state, Eq. (47) can be written as $s_k = H^{-1} Q_r r_k$, where $H = \Phi^T - (\Phi^T P \Gamma + N_d)\bar{R}_d^{-1}\Gamma^T - I$ and where $P = P_k = P_{k+1}$. Now the optimal control Eq. (45) can be rewritten as $u_k = F x_k + G r_k$, with

$$F = -\bar{R}_d^{-1}\left(\Gamma^T P_k \Phi + N_d^T\right)$$

and

$$G = -\bar{R}_d^{-1}\left(\Gamma^T H^{-1} Q_r - N_d^T L\right) \tag{A8}$$

where F is the feedback gain and G is the feed-forward gain.

References

[1] Utkin, V. I., *Sliding Modes and Their Application in Variable Structure Systems*, Mir Publishers, Moscow, 1978, Chap. 1–3.

[2] Decarlo, R. A., Zak, S. H., and Mathews, G. P., "Variable Structure Control of Non-Linear Multivariable Systems: A Tutorial," *Proceedings of the IEEE* , Vol. 76, No. 3, 1988, pp. 212–232.

[3] Hung, J. Y., Gao, W., and Hung, J. W., "Variable Structure Control: A Survey," *IEEE Transactions on Industrial Electronics*, Vol. 40, No. 1, 1993, pp. 2–22.

[4] Gao, W., and Hung, J. C., "Variable Structure Control of Non-Linear Systems: A New Approach," *IEEE Transactions on Industrial Electronics*, Vol. 40, No. 1, 1993, pp. 45–55.

[5] Furuta, K., "Sliding Mode Control of a Discrete System," *Systems and Control Letters*, Vol. 14, No. 2, 1990, pp. 145–152.

[6] Gao, W., Wang, Y., and Homaifa, A., "Discrete-Time Variable Structure Control Systems," *IEEE Transactions on Industrial Electronics*, Vol. 42, No. 2, 1995, pp. 117–122.

[7] Sarpturk, S. Z., Istefanopulos, Y., and Kaynak, O., "On the Stability of Discrete-Time Sliding Mode Control Systems," *IEEE Transactions on Automatic Control*, Vol. 32, No. 10, 1987, pp. 930–932.

[8] Koshkouei, A. J., and Zinober, A. S. I., "Sliding Lattice Design for Discrete-Time Linear Multi-Variable Systems," *Proceedings of the 35th IEEE Conference on Decision and Control*, Vol. 2, IEEE Press, New York, 1996, pp. 1497–1502.

[9] Edwards, C., and Spurgeon, S. K., "Robust Output Tracking Using a Sliding Mode Controller/Observer Scheme," *International Journal Control*, Vol. 64, No. 5, 1996, pp. 967–983.

[10] Spurgeon, S. K., "Hyperplane Design Techniques for Discrete-Time Variable Structure Control Systems," *International Journal Control*, Vol. 55, No. 2, 1992, pp. 445–456.

[11] Tang, Y. C., and Misawa, A. E., "Sliding Surface Design for Discrete VSS Using LQR Technique with a Preset Real Eigen Value," *Systems and Control Letters*, Vol. 45, No. 1, 2002, pp. 1–7.

[12] Elmali, H., and Olgac, N., "Sliding Mode Control with Perturbation Estimation (SMCPE): A New Approach," *International Journal Control*, Vol. 56, No. 2, 1992, pp. 923–941.

[13] Chan, C. Y., "Robust Discrete-time Sliding Mode Controller," *Systems and Control Letters*, Vol. 23, No. 5, 1994, pp. 371–374.

[14] Eun, Y., and Cho, D. D., "Robustness of Multivariable Discrete-Time Variable Structure Control," *International Journal Control*, Vol. 72, No. 12, 1999, pp. 1106–1115.

[15] Furuta, K., and Pan, Y., "Variable Structure Control with Sliding Sector," *Automatica*, Vol. 36, No. 2, 2000, pp. 211–228.

[16] Cheng, C. C., Lin, M. H., and Hsiao, J. M., "Sliding Mode Controllers Design for Linear Discerte-Time Systems with Matching Perturbations," *Automatica*, Vol. 36, No. 8, 2000, pp. 1205–1211.

[17] Chen, M. S., Hwang, Y. R., and Tomizuka, M., "A State-Dependent Boundary Layer Design for Sliding Mode Control," *IEEE Transactions on Automatic Control*, Vol. 47, No. 12, 2002, pp. 1677–1681.

[18] Garnell, P., *Guided Weapon Control Systems*, 2nd ed., Pergamon, New York, 1980, pp. 37–151.

[19] Salamci, M. U., and Ozgoren, M. K., "Sliding Mode Control with Optimal Sliding Surfaces for Missile Autopilot Design," *Journal of Guidance, Control, and Dynamics*, Vol. 23, No. 4, 2000, pp. 719–727.

[20] Thukral, A., and Innocenti, M., "A Sliding Mode Missile Pitch Autopilot Synthesis for High Angle of Attack Maneuvering," *IEEE Transactions on Control Systems Technology*, Vol. 6, No. 3, 1998, pp. 359–371.

[21] Bhat, S. M., Bai, S. D., Powly, A. A., Swamy, K. N., and Ghose, D., "Variable Structure Controller Design with Application to Missile Tracking" *Journal of Guidance, Control, and Dynamics*, Vol. 24, No. 4, 2001, pp. 859–862.

[22] Elbrous, M. J., and Ramazan, T., "Design of Robust Autopilot-Output Integral Sliding Mode Controllers for Guided Missile Systems with Parameter Perturbations," *Aircraft Engineering and Aerospace Technology*, Vol. 73, No. 1, 2001, pp. 16–25.

[23] Wang, J., Brussel, H. V., and Swevers, J., "Robust Perfect Tracking Control with Discrete Sliding Mode Controller," *Journal of Dynamical Systems, Measurement and Control*, Vol. 125, No. 1, 2003, pp. 27–32.

[24] Anderson, B. D. O., and Moore, J. B., *Optimal Control: Linear Quadratic Methods*, Prentice–Hall, Upper Saddle River, NJ, 1989, pp. 68–100.

[25] Hill, D. J., and Moylan, P. J., "Dissipative Dynamical Systems: Basic Input-Output and State Properties," *Journal of The Franklin Institute*, Vol. 309, No. 5, 1980, pp. 327–357.

[26] Kuo, B. C., *Digital Control Systems*, Holt, Rinehart and Winston, Philadelphia, 1980, pp. 601–638.